LAWRENCE
LIVERMORE
NATIONAL
LABORATORY

LLNL-PROC-559642

Influence of Mechanical Properties Relevant to Standoff Deflection of Hazardous Asteroids

I. Lomov, E. B. Herbold, T. H. Antoun, P. Miller

June 4, 2012

2012 Hypervelocity Impact Symposium
Baltimore, MD, United States
September 16, 2012 through September 20, 2012

Disclaimer

Influence of Mechanical Properties Relevant to Standoff Deflection of Hazardous Asteroids

Ilya Lomov,* Eric B. Herbold, Tarabay H. Antoun, and Paul Miller

Lawrence Livermore National Laboratory, L-236,

P.O. Box 808, Livermore, CA 94550, U.S.A.

(Dated: June 4, 2012)

Abstract

National Academy produced reports on the potential hazard and mitigation strategies for near Earth objects (NEO) [9, 10]. The NRC reported to Congress that nuclear explosives are the only current technology to protect the Earth from impact from large asteroids. This is mainly due to difficulties in predicting the impact with high confidence leading to a short time to impact. Thus, the velocity deflection required when they are determined to be potentially hazardous asteroids (PHA) can only be achieved with nuclear explosives. A standoff explosion, without direct contact with the Near Earth Object (NEO) is a robust option for soft non-destructive push, which offers several advantages. We have investigated the efficiency of energy deposition dependence on porosity and strength properties of NEO. A Eulerian hydrocode (GEODYN) with an interface reconstruction algorithm, wide-range equation of states and a flexible constitutive model library was used for numerical studies. The largest difficulties in predicting deflection velocity and fragmentation of asteroids are related to uncertainty in composition and mechanical properties of NEO. To reduce this uncertainty, we performed simulations of normal impact cratering of an NEO surface and related results with observables such as the crater shapes, the critical crater diameter (necessary to iron-out previous craters) and the maximum crater size (necessary for asteroid break-up). The velocity distribution of the material ejected from the impact crater is also germane to the asteroid deflection problem where the ablated material provides the thrust resulting in a deflection velocity. We performed parametric studies on how porosity and strength of the asteroid would affect these results.

PACS numbers:

*Electronic address: lomov@llnl.gov

I. INTRODUCTION

There are several proposed methods for deflecting asteroids of a size greater than 50m. At this diameter, an asteroid or meteor impact with the earth would adversely affect all human life. As detection methods improve, more and more potentially hazardous asteroids are found and tracked. Though we many know the size and trajectory of these bodies, very little is known about the composition of the mass (e.g. is it composed of competent rock, ice, mixed, etc.). Most impulsive methods proposed to change the course of these planetary bodies rely on pushing the asteroid from one side. Depending on how far away the asteroid may be when it is determined to be on a crash course with the earth, we may or may not have time to wait for the asteroid to change paths. How feasible, then, is it to break up an asteroid? How should this be done without knowing anything about the internal composition of the asteroid?

II. NUMERICAL MODEL

The simulations presented in this paper are conducted using GEODYN – a parallel Eulerian compressible solid and fluid dynamics code with adaptive mesh refinement (AMR) capabilities [1, 6]. Among its many features are a high-order material interface reconstruction algorithm [4] and advanced constitutive models that incorporate salient features of the dynamic response of geologic media [11]. GEODYN is able to simulate materials under extremely large deformations, resolve details of wave propagation within grains with high accuracy, and uses a continuum damage mechanics approach to represent fracture.

The Eulerian framework of adaptive mesh refinement [3] is a relatively mature technique for dynamically applying high numerical resolution to those parts of a problem domain that require it, while solving less sensitive regions on less expensive, coarser computational grids. Adaptive mesh refinement can help to simulate the entire process region (or a significant portion thereof) while allowing focus on greater details in interesting locations. In combination, Eulerian Godunov methods with AMR have been proven to produce highly accurate and efficient solutions to shock capturing problems. The method used here is based on some modifications of the single-phase high-order Godunov method. This method is not as straightforward as Lagrangian FEM, so it will be briefly summarized below. For solid

mechanics, the governing equations consist of the laws of conservation of mass, momentum and energy, an equation for distortional elastic deformation, and a number of equations in a form of

$$\frac{\partial}{\partial t}\left(\rho F_i\right) + \nabla \cdot \left(\rho \mathbf{v} F_i\right) = \rho \Phi_i, \tag{1}$$

which represent specific rheological equations $\dot{F}_i = \Phi_i$ (a superposed dot denotes material time differentiation) for history dependent parameters F_i (like porosity, plastic strain, etc.). The viscoplasticity is modelled with a measure of elastic deformation as a symmetric, invertible, positive definite tensor $\mathbf{B}_e$, which is determined by integrating the evolution equation

$$\dot{\mathbf{B}}'_e = \mathbf{L} \cdot \mathbf{B}'_e + \mathbf{B}'_e \cdot \mathbf{L}^\top - 2/3\mathbf{L} : \mathbf{I} - \mathbf{A}_d \,, \tag{2}$$

where $\mathbf{L}$ denotes the velocity gradient [12]. It is possible to define a unimodular tensor which is a pure measure of elastic distortional deformation $\mathbf{B}'_e$. In traditional von Mises materials shear stresses depend purely on $\mathbf{B}'_e$. The inelastic deviatoric deformation tensor $\mathbf{A}_d$ can be written as:

$$\mathbf{A}_d = \Gamma_d \left(\mathbf{B}'_e - \left(\frac{3}{\mathbf{B}'_e : \mathbf{I}} \right) \mathbf{I} \right) \,, \tag{3}$$

where the scalar rate functions Γ_d require constitutive equations. The rate-dependent formulation (3) can be easily converted to a rate-independent von Mises functional form.

The numerical scheme for a single fluid cell is based on the approach of Miller [8], with some modifications to account for the full stress tensor associated with solids. The multidimensional equations are solved by using an operator splitting technique, in which the one-dimensional equations for each direction are solved:

$$U^{n+2}_{i,\alpha} = S_H \left(S_{0,0,1} \left(S_{0,1,0} \left(S_{1,0,0} \left(S_H \left(S_{1,0,0} \left(S_{0,1,0} \left(S_{0,0,1} \left(U^n_{i,\alpha} \right) \right) \right) \right) \right) \right) \right) \right) \,, \tag{4}$$

where the spatially split operators

$$S_{i_\beta, j_\beta, k_\beta} \left(U^{n+m/3}_{1,\ldots,l,\alpha} \right) \tag{5}$$

are applied in a Strang-splitting order to keep second-order accuracy, while the source term

$$S_H \left(U^{n,H}_{1,\ldots,l,\alpha} \right) = U^{n,H}_{1,\ldots,l,\alpha} + \Delta t V_\alpha H_\alpha \left(U^{n,H}_{1,\ldots,l,\alpha} \right) \tag{6}$$

is always applied at the end of the timestep. Each directional operator is the update of the cell from time step n to time step n+1 with fluxes computed at the cell's edges. Edge fluxes

are calculated based on upwind characteristic tracing following Miller [8] and to Riemann solver in an acoustic approximation. The estimate for the velocity gradient L in (6) is calculated in the Riemann solver step.

The biggest challenge in the Eulerian and multimaterial ALE methods is the treatment of mixed cells that contain several materials. The algorithm described here treats the propagation of surfaces in space in terms of an equivalent evolution of volume fractions defined by the equation:

$$\frac{\partial f_\alpha}{\partial t} + \nabla \cdot (f_\alpha \mathbf{v}) = \frac{f_\alpha}{K_\alpha} K \nabla \cdot \mathbf{v}, \tag{7}$$

where f_α and K_α are the volume fraction and the bulk modulus of each material α. The approach to modelling multimaterial cells is similar to that in Miller [8]. Specifically, material properties have multiple values in a cell, but the velocity and stress are single-valued. In order to use the single-fluid solver, it is necessary to define an effective single phase for the mixed cells and to update material volume fractions based on self-consistent cell thermodynamics:

$$\begin{aligned} 1/K &= \sum f_\alpha / K_\alpha \qquad & T_{ii} &= 1/K \sum f_\alpha T_{ii\alpha}/K_\alpha \\ 1/G &= \sum f_\alpha / G_\alpha \qquad & T_{ij,i\neq j} &= 1/G \sum f_\alpha T_{ij\alpha}/G_\alpha \end{aligned} \tag{8}$$

where $G_\alpha, T_{ij\alpha}$ are the shear modulus and the stress tensor of material α. Distribution of the velocity gradient amongst each material in the cell required to integrate (2) for each material is done in a similar way:

$$\mathbf{L}_\alpha = \mathbf{L} G / G_\alpha \,. \tag{9}$$

In order to advect volume fractions, we use a high order interface reconstruction (interface tracking), which preserves linear interfaces during translation. Constraint on volume fractions is satisfied assuming fast equilibration of partial pressures in the cell. The pressure relaxation algorithm consists of iterative adjustments of volume fractions. First, average pressure is calculated:

$$p = \sum_\alpha \frac{f^\alpha p^\alpha}{K^\alpha} \Bigg/ \sum_\alpha \frac{f^\alpha}{K^\alpha} \ . \tag{10}$$

Next, the change of volume fraction for current iteration step is calculated:

$$\delta f_\alpha = \beta_\alpha f_\alpha (p^\alpha - p) \,./ K^\alpha \tag{11}$$

The limiter β_a in (11) is chosen from numerical and physical considerations, i.e. all volume fractions should fall in the zero to one range, change of material density should be limited, etc.

III. 3D SIMULATION OF DEFLECTION AND FRAGMENTATION OF AN ASTEROID BY A STANDOFF NUCLEAR EXPLOSION

One of most efficient and robust ways to deflect NEO is a standoff nuclear explosion. Energy from neutron and x-ray deposition heats a surface layer of asteroid and generate fast fluid ejecta, which pushes most of the astroid mass in the opposite direction. Neutrons are more efficient per delivered energy than x-rays since their mean free path in solids are longer. Thus, neutron ejecta has more mass at lower velocities, which leads to higher momentum per given energy density [7, 13]. In this paper, we consider a hypothetical neutron source with mean free path in asteroid material λ=0.3m. Figure 1 show results of 3D simulation of a nuclear explosion near an asteroid. The one of the purposes of the simulation was to evaluate damage to the asteroid body by such an explosion. To eliminate artifacts of the solution related to symmetric shape, we used a scaled version of the Geographos asteroid. For material model, we used a fairly complicated model calibrated by fractured granite response to penetration and wave propagation [14]. To represent a standoff 750kt nuclear explosion we assume 150kt of deposited energy acting upon an asteroid volume equivalent to a 500-meter-diameter sphere. The finest mesh resolution in these 3D simulation was 0.75m, which was not adequate for resolving details of the ablated layer. Consequently, we further simplified initial condition, assuming an ideal gas equation of state in the ablated layer with initial energy density 2.5MJ/kg.

The resulting bulk deflection velocity is about 0.6m/s. Component of the velocity records along the direction connecting the centers of the asteroid and explosion are presented on Fig. 2. Damage patterns presented on Fig. 1 with black color and dispersion of velocities presented on 1 suggest full fragmentation of this relatively strong asteroid under simulated conditions. On the other hand, the simulation show that the velocity variations are somewhat smaller that escape velocity (approximately 0.3m/s), so most likely most of the asteroid fragments will stay together. Relative motion will eventually dissipate in fragment collisions, forming a rubble pile. The case considered in this section present an upper limit for the usual range of desired deflection velocities in the planet defence literature. Deflection velocities of 0.01m/s and even lower can be sufficient if NEO intercepted months or years in advance. Such scenarios are not likely to break an asteroid into dispersing cloud.

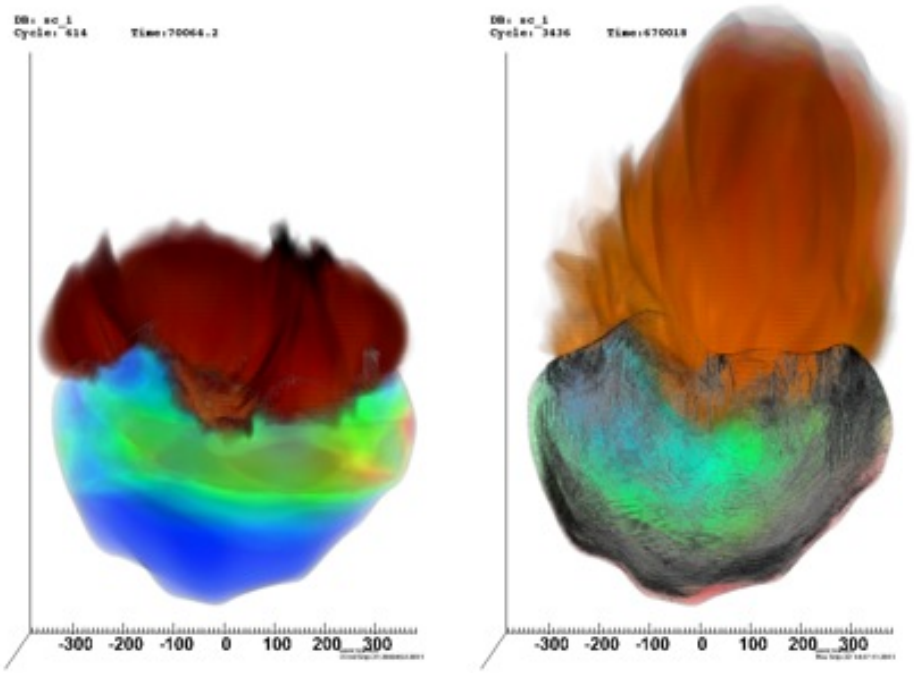

FIG. 1: Two visualizations are presented from the calculation of the response of a scaled version of the Geographos asteroid to a standoff 750kt nuclear explosion. The simulation represents 150kt of deposited energy acting upon an asteroid volume equivalent to a 500-meter-diameter sphere. Image times are 0.07s (left) and 0.67s (right). Each graphic combines volume rendering of three quantities: energy density in the ejecta (orange colorscale), velocity (RGB colorscale) and damage (grey scale).

IV. INFLUENCE OF MATERIAL POROSITY ON MOMENTUM FROM NUCLEAR BLOW-OFF

There is very little information about NEO material properties. Usually only bulk density, temperature and composition can be derived from observations. Given scarcity of such data, simulation of asteroid-related impacts and similar events usually restricted to very simple, if any, models for rock strength, damage and porosity compaction. In many cases, where results are mostly affected by regions loaded above 10 GPa pressures, such assumptions may be justified. On the other hand, standoff nuclear explosion may not generate so extreme pressures that strength effects can be ignored in simulations of the neutron ejecta. Moreover, simple analysis show that very porous materials may not generate strong ejecta

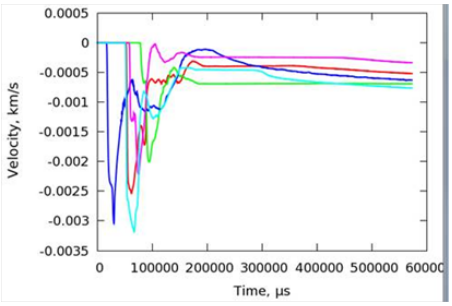

FIG. 2: Velocity records in various locations in asteroid

until completely evaporated and also may shield inner regions of the asteroid from the vapor pressure generated on the surface. For instance, in the extreme case of no resistance to porosity compaction ("snow-plow" model, which is often used in hydrocodes) there will be no pressure build-up and ejecta until all pressure will be closed due to thermal expansion.

A. Simulations with continuum model for macroporosity

To evaluate effects of porosity to momentum delivered to the bulk of the asteroid, we conducted one-dimensional studies of pressure wave propagation in porous material. The energy is assumed to be deposited by neutrons with mean free path of λ=0.3m, exponentially decaying from the surface. Earlier results from [7, 13] show that for non-porous asteroid, a 7.3kT nuclear explosion at the optimal stand-off distance $d = 1/3R_a$ (R_a is the asteroid radius) can generate 0.1m/s deflection velocity for an asteroid with 500 meter diameter. Such an explosion deposits energy ϵ_0=0.62MJ/kg on the surface point closest to the explosion. The value of ϵ_0 is used as reference energy for 1D parametric studies presented here. We studied dependence of momentum delivered to the bulk of the asteroid on two key parameters of porosity model: initial porosity Φ and the compaction slope s ($s = 1$ corresponds to the snow plow model; $s = 0$ is the fully elastic, no compaction case). "Bulk" or "average" density, which is usually known with higher accuracy then "solid" density, has been fixed in the studies to $\rho_0 = 1.876g/cm^3$. Accordingly, the solid density (the equation of state parameter) is changing with porosity. The compaction slope s is the most important parameter of the compaction model. For a given rock type, geomaterials show some correlation between initial porosity and compaction slope, but there is no universal correlation between them,

i.e. there could be weak low-porosity as well as strong high porosity rocks and effects of those two parameter should be studies independently. There are other parameters of compaction model which can influence the material response (onset of compaction, stiffening at higher pressures, shear-enhanced compaction), but their effects can be partially evaluated by variation of Φ and s and beyond the current study. Figure 3 represents influence of the porosity model on the deflection momentum. It is clear that even less than 10% porosity, which is very likely to be present in asteroid, can significantly reduce the deflection velocity. At high porosity values, there is still some deflection velocity present, which is explained by the fact that deviatoric strength model has been fixed in this parametric study. In reality, for highly porous, volumetrically soft material deviatoric strength will also be low, which also reduce the deflection velocity. Figure 3 also show monotonic velocity dependence on the compaction slope s. For most porous geologic materials initial compaction slope varies from 0.6 to 0.98, so deflection velocity is quite sensitive to this parameter, which depends not only on mineral composition, but also material morphology.

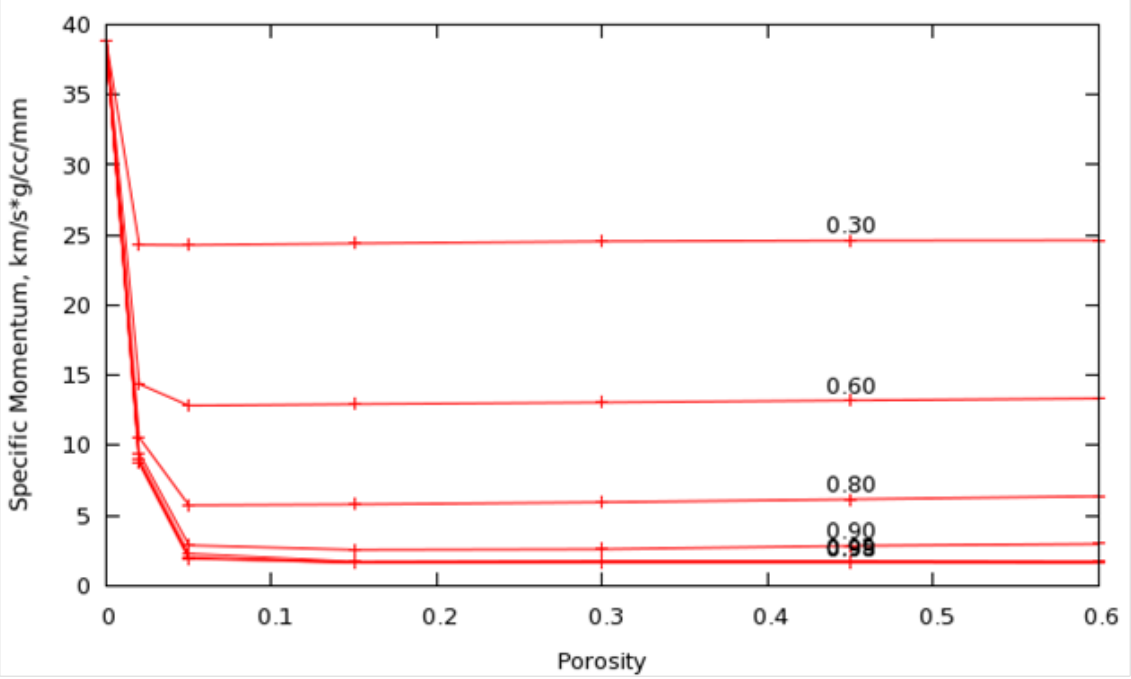

FIG. 3: Porosity effect on 1D momentum transmitted into the body of the asteroid. Numbers on top of the each line indicate the compation slope s.

Results of this parametric study show that explosion at the optimal (from the pure

hydrodynamic considerations) stand-off distance $d = 1/3R_a$ near porous NEO may create too low energy density in the blow-off layer. The deflection velocity can be reduced more than ten-fold. Only when ϵ_0 significantly exceeds the cohesive energy of material (about 5MJ/kg for many rock types), pressure becomes relatively insensitive to mass density (vs. energy density) and details of material strength would not matter. To eliminate this uncertainty, it may be required to reduce the stand-off distance of the explosion and increase ϵ_0.

B. Boulder-resolving simulations of blow-off layer

Large uncertainty of deflection velocity on asteroid porosity observed in the simulations with a phenomenological model can be addressed if we can constrain compaction behavior. If fragment size distribution and composition of asteroid surface is available, it is possible to run a fragment-resolving mesoscale simulation of the energy deposition and establish the lower bound of the compaction curve for a given morphology and composition. Even in the one of the "worst-case" scenarios with high initial porosity $\Phi = 45\%$ and no material strength (which would correspond to a snow-plow continuum model) local heterogeneities of the pressure field generate chaotic motion of the fragments which later converts to coherent motion in the blow-off direction. For the standard case considered in the previous section ϵ_0=0.62MJ/kg the average ejecta velocity reaches 75m/s which is comparable to ejecta velocity in non-porous material. Figure 4 illustrates initial and final density plots of asteroid material. The fragments are initialized as monodispersed polyhedra with an average size $D_p = \lambda/10$. The deflection velocity should depend on initial particle size distribution, the ratio D_p/λ, strength of the individual fragments and is subject of the ongoing mesoscale studies.

V. ASTEROID CHARACTERIZATION FROM HYPERVELOCITY IMPACT CRATERING AND RESURFACING

Since porosity of asteroid is of one of the most important parameters for nuclear energy deposition, it is important to relate it to one of the few characteristics of the asteroid - hypervelocity impact craters. We will study this relationship on the example of the Stickney crater on Phobos, which creation has been modeled before [2]. Mariner-9 and Vikings

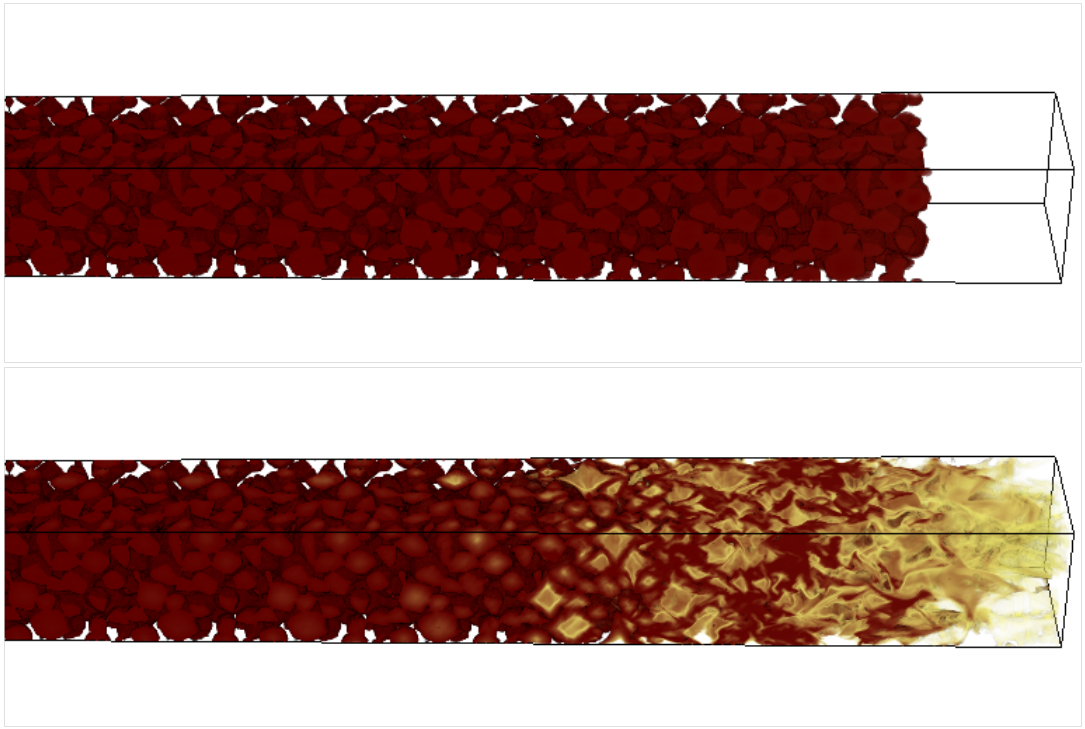

FIG. 4: Mesoscale simulations of material expansion after instantaneous energy depostion. Initial and final density fields are shown.

photometry show Phobos as an asteroid-like dark celestial body [5]. Large impact events, like Stickney creation, can resurface an asteroid. Critical diameter, which defined as the smallest crater whose formation disrupts all previous craters globally up to its size, is most likely also influenced by asteroid porosity. In this section we will only focus on 2D axisymmetric simulations. Moreover, final crater shape and asteroid surface may be affected by slow gravity-driven motions, which are hard to simulate accurately in hydrocodes. So, we will look on the issue of resurfacing only by considering whether it is possible to disrupt relatively intact, cohesive asteroid surface. In this case, the metric for resurfacing of the asteroid is damage of the asteroid surface and significant (but not necessarily higher than escape) fragment velocities.

The initial conditions for simulation are set similar to [2]. The impact velocity was 8.3km/s, $R_{Phobos} = 11km$. In all simulations we used quite complicated geologic cap model [14]. In order to see the effects of constitutive models, without changing extensive quantities like volume and mass, we used Mie-Gruneisen equation of state, which is easier to

parameterize. To evaluate effects of different equations of state, we performed the baseline simulation did not include initial porosity, with both Mie-Gruneisen and table equations of state for granite. Plots on Fig. 5 show that while there is significant difference in the ejecta shape, there is very little difference in the damage pattern.

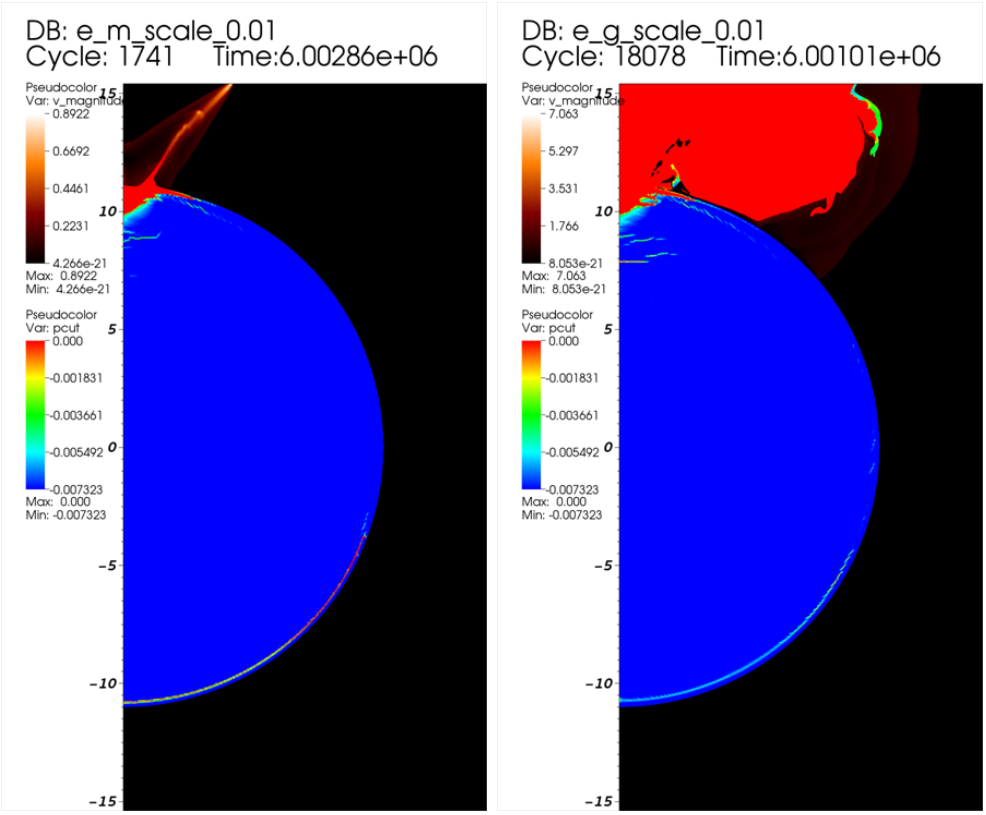

FIG. 5: Simulations of impact generated Stickney crater on Phobos. $R_{impactor} = 0.01R_{Phobos}$ Snapshots of material damage 6 seconds after impact. Left: Mie-Gruneisen EOS Right: Table (Granite) EOS.

Effects of the size of the impactor in non-porous case are shown on Fig. 6. For the case of $R_{impactor} = 0.02R_{Phobos}$ the size of the completely damaged zone near the crater is comparable to the final crater shape. Material in this zone still has significant velocities at the end of the simulation, such that it is likely that it most of it can eventually leave the crater region, forming a crater, similar in size to an observable. Most of the asteroid surface is spalled by a reflected tensile wave and the surface fragments have significant radial velocities which would completely resurface the asteroid. Interestingly, for smaller impactor $R_{impactor} = 0.01R_{Phobos}$, the spall is formed mostly on the back side of the asteroid,

suggesting that it is more susceptible to partial resurfacing for non-porous asteroids. Another characteristic of non-porous resurfacing is that most of the damage is spall-related, besides relatively small surface right next to the impact event.

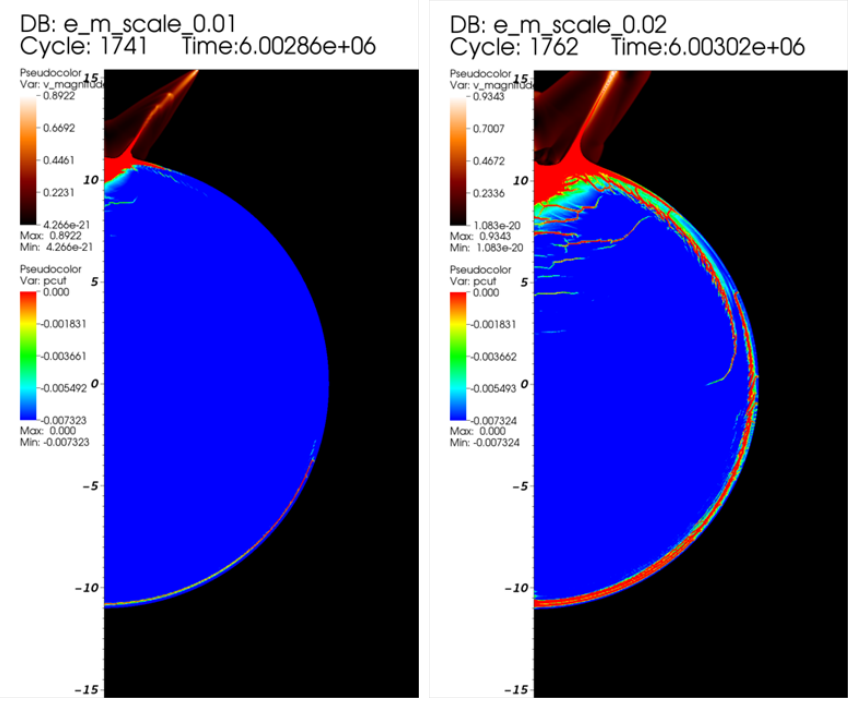

FIG. 6: Simulations of impact generated Stickney crater on Phobos. Snapshots of material damage 6 seconds after impact. Left: $R_{impactor} = 0.01 R_{Phobos}$ Right: $R_{impactor} = 0.02 R_{Phobos}$.

Figure 7 represents effect of porosity on the initial crater shape and damage pattern. Simulations show that craters in porous asteroids tends to have higher depth to width ratio than in non-porous. Undoubtedly, the quantitative comparisons between simulated crater shape at 6 seconds after impact and observations are not possible because of late-time motion, but this correlation can be used for asteroid characterization among other criteria. Case of 20% porous asteroid seemed to have the smallest damage surface area. This is explained by stronger wave attenuation, compared to the non-porous case from one side, and on the other side, it is still relatively strong and can support some load before damage, unlike higher-porosity (30%) case. Of course, this peak of the damaged surface area of the asteroid is related to choice of material parameters and may or may not exist for other correlations between initial porosity and material strength. Partial resurfacing of porous asteroids tend to happen on the regions of asteroid close to impact site due to fast

attenuation of the shock waves in the porous medium and long and smooth pulse, which is not capable to produce spall. Thus, most of the damage in porous asteroids are compaction or shear related, rather then tensile. If it is possible to correlate partially resurfaced areas of the asteroid with a particular impact crater, they should be collocated on highly-porous astedoids and be on the opposite sides on non-porous asteroids.

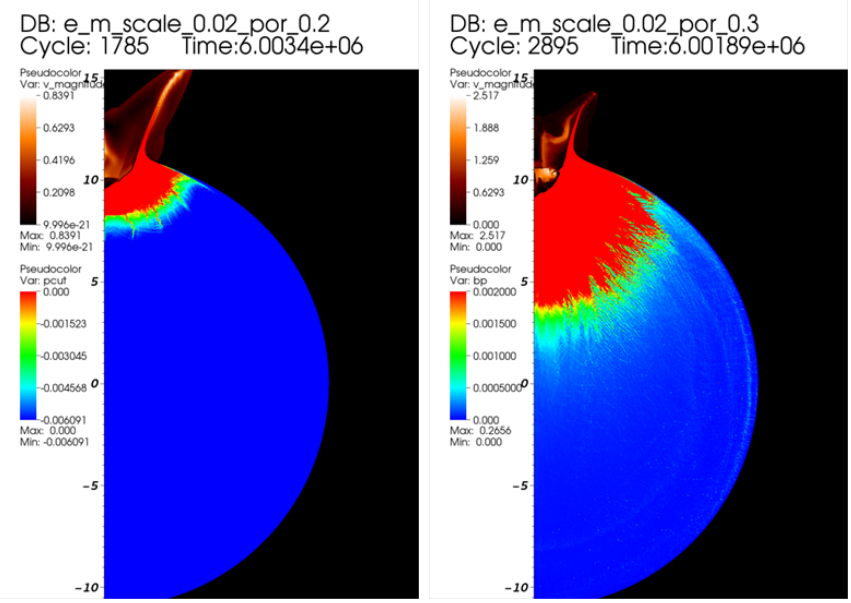

FIG. 7: Simulations of impact generated Stickney crater on Phobos. Snapshots of material damage 6 seconds after impact. $R_{impactor} = 0.02 R_{Phobos}$. Left: $\Phi = 20\%$ Right: $\Phi = 30\%$.

VI. CONCLUSIONS

Standoff nuclear explosion is a viable option to mitigate hazardous NEOs. An attempt to deflect NEO can also fragment it. Nevertheless, the velocity dispersion of individual fragments are not large than the average deflection velocity. Accordingly, for all but the very high deflection velocities (comparable to the escape velocity of the asteroid), even if fragmented, the fragments will travel as a rubble pile after the deflection event. Simulations of ejectas generated by energy deposited from nuclear blasts show that deflection velocities can strongly depend on the asteroid material properties. Variations of phenomenological material model for porous asteroid show possible ten-fold decrease of deflection velocities in certain scenarios. In order to reduce this uncertainty it may be required to change engage-

ment parameters from otherwise more optimal. The other way to reduce this uncertainty is to constrain the set of parameters of material models. We presented two approaches to achieve this goals. The first approach is to proceed with mesoscale simulations, restricting possible morphology and properties of non-porous mineral. Preliminary study show that even in some worst-case scenarios it is possible to reduce the uncertainty of the phenomenological models. The second approach is to correlate observable craters on the asteroids with simulations of impact craters under different impact conditions and material properties. Some geometric observables (crater aspect ratio, location of resurfaced areas relative to impact site, differentiation between spall and shear damage) can be used to narrow down parameters of the porosity compaction model.

Acknowledgments

This work was performed under the auspices of the U.S. Department of Energy by Lawrence Livermore National Laboratory under Contract DE-AC52-07NA27344.

---

[1] T. H. Antoun, I. N. Lomov, and L. A. Glenn. Development and application of a strength and damage model for rock under dynamic loading. In D. Elsworth, J. Tinucci, and K. Heasley, editors, *Proceedings of the 38th U.S. Rock Mechanics Symposium, Rock Mechanics in the National Interest*, pages 369–374. A. A. Balkema Publishers, 2001.

[2] E. Asphaug and H.J. Melosh. The Stickney Impact of Phobos: A Dynamical Model. *Icarus*, 101:144, 1993.

[3] M. J. Berger and P. Colella. Local adaptive mesh refinement for shock hydrodynamics. *Journal of Computational Physics*, 82(1):64–84, May 1989.

[4] E. S. J. Hertel and R. L. Bell. *An improved material interface reconstruction algorithm for Eulerian codes.* Sandia Nat Lab, 1992.

[5] E Illes, A Horvath, F Horvath, and A Gesztesi. IN SITU MEASUREMENTS TO DETERMINE IF PHOBOS IS LAYERED. *Acta Astronautica*, 12(6):602, 1985.

[6] I. Lomov and M.B. Rubin. Numerical simulation of damage using an elastic-viscoplastic model with directional tensile failure. *Journal De Physique IV*, 110:281–286, 2003.

[7] A. Miles and J. Sanders. Mitigation of Earth-asteroid collisions via explosive, intense radiation sources. In *APS Meeting Abstracts*, page 1172P, October 2005.

[8] G. H. Miller and E. G. Puckett. A high-order godunov method for multiple condensed phases. *Journal of Computational Physics*, 128(1):134–164, Oct 1 1996.

[9] NAS. *Near-Earth Object Surveys and Hazard Mitigation Strategies : Interim Report Committee to Review Near-Earth Object Surveys and Hazard Mitigation*. 2009.

[10] NAS. *Defending Planet Earth : Near-Earth Object Surveys and Hazard Mitigation Strategies Committee to Review Near-Earth Object Surveys and Hazard Mitigation Strategies ; National Research Council*. 2010.

[11] M. B. Rubin and I. Lomov. A thermodynamically consistent large deformation elastic-viscoplastic model with directional tensile failure. *International Journal of Solids and Structures*, 40(17):4299 – 4318, 2003.

[12] M. B. Rubin, O. Y. Vorobiev, and L. A. Glenn. Mechanical and numerical modeling of a porous elastic-viscoplastic material with tensile failure. *International Journal of Solids and Structures*, 37(13):1841–1871, Mar 2000.

[13] J. C. Sanders. *Near Earth Object Collisional Mitigation Via Intense Neutron and Photon Sources: a Study in Asteroid Interdiction and Energy Coupling*. PhD thesis, Oregon State University, 2006.

[14] O. Y. Vorobiev, B. T. Liu, I. N. Lomov, and T. H. Antoun. Simulation of penetration into porous geologic media. *International Journal Of Impact Engineering*, 34(4):721–731, Apr 2007. 0734-743X.